Electrochimica Acta, Vol 37, No 4, pp 655–663, 1992
Printed in Great Britain

0013-4686/92 $5 00 + 0 00

THE FORMATION OF ANODIC LAYERS ON ANNEALED COPPER SURFACES IN PHOSPHATE-CONTAINING SOLUTIONS AT DIFFERENT pH

M M LAZ, R M SOUTO, S GONZÁLEZ, R C SALVAREZZA* and A J ARVIA*
Departamento de Química Física, Universidad de La Laguna, Tenerife, Spain

(*Received* 28 *May* 1991, *in revised form* 11 *July* 1991)

Abstract—The electrochemical behaviour of Cu in different phosphate buffers is studied through electrochemical techniques combined with scanning electron microscopy and energy dispersive X-ray analysis At pH 6 0 and 8 0 the onset of passivation is due to the anodic formation of a basic Cu(II) phosphate, whereas at pH 11 5 the passivating layer corresponds to a duplex Cu(I) oxide–Cu(II) oxide layer The potentiostatic anodic current transients can be reproduced by a model involving the initial growth of a thin anodic layer and the simultaneous electrodissolution of Cu The electrodissolution of passivated Cu takes place through the passivating layer This reaction contributes to the thickening of the outer part of the passivating layer

Key words anodic layers, copper passivation, phosphate solutions, growth mechanism, duplex-type passive layers

1. INTRODUCTION

The study of the electrochemical behaviour of Cu in phosphate-containing solutions has been mainly focussed on Cu electropolishing in concentrated phosphoric acid[1–6] Different aspects of this process such as the contribution of transport processes[7, 8], the formation of anodic layers[9–14], and the appearance of photoeffects during electropolishing[15–19] have been investigated by employing different electrochemical and surface analysis techniques Nevertheless, there are still a number of problems emerging from the inherent complexity of the system which remain open for further research work

A detailed survey of the literature, particularly that corresponding to the current–potential curves shows that Cu pitting and Cu electropolishing appear as two processes which are to some extent interrelated, at least within a certain transition potential range Furthermore, the kinetics of the corrosion and passivation of relatively soft metals such as Cu, in addition to the influence of the electrolyte solution composition, depends also on the initial metallurgical and mechanical treatments of the specimens. For a clear understanding of these questions a systematic work in different electrolytes with a standardized Cu specimen is necessary

The present work is devoted to investigating the reactions related to the anodization of Cu in phosphate-containing buffered solutions at different pH values, and to determine the type of anodic layers which are formed under different conditions.

*Visiting Professor, Consejo Nacional de Investigaciones Científicas y Técnicas, Argentina

2. EXPERIMENTAL

The working electrodes were made from 99 9% purity electrolytic polycrystalline Cu rods Each specimen was machined in the lathe from drawn Cu bars of 1/4 inch diameter to obtain cylindrical specimens The actual working electrode active area was the base of a small Cu cylinder of 0 3 cm diameter which was mounted as a horizontal disc electrode in contact with a hanging electrolyte column[20] by fixing the height of the meniscus to 5 mm from the solution level This arrangement could be used under either a stagnant solution condition or with stirring up to 5000 rpm Each working electrode was firstly mechanically polished, then thermally treated, and finally, subjected to electropolishing

The mechanical treatment comprised a sequential polishing with different grain size emery papers up to 1 μm grit diamond paste The specimens were then repeatedly rinsed with distilled water, and finally dried in air

To assure good reproducibility of results annealed Cu specimens were used Therefore, the specimens were annealed at 500°C for 2 h[21] to eliminate residual mechanical stresses and to produce a relatively more uniform grain distribution in the metal. For this purpose a number of Cu specimens were lodged in a Pyrex tube which was repeatedly swept with Ar using a vacuum line, and then sealed off with a residual Ar pressure of about 1–2 Torr The heating and cooling rates employed for annealing were 500°C h^{-1}, and 80–100°C h^{-1}, respectively

The electropolishing of annealed Cu specimens was made in stagnant ortho-phosphoric acid (1 71 g cm^{-3}) at 0 3 A cm^{-2} and room temperature

In this case a large Cu plate counter electrode parallel to the small Cu disc electrode surface was employed to achieve a reasonably good primary current distribution in the cell The electropolishing time was varied from 5 to 10 min

Finally, the treated Cu specimens were rinsed repeatedly with twice-distilled water The surface finishing was checked by reflection and scanning electron microscopies

Electrochemical runs were made in a conventional three-electrode Pyrex glass cell The counter electrode was a large area Pt screen placed around the working electrode The reference electrode was a saturated sodium chloride/calomel electrode (*ssce*) The latter was connected to the cell through a conventional Luggin capillary arrangement filled with the electrolyte solution Runs were made at 25 0 ± 0 1°C in the following electrolyte solutions (i) x M Na_2HPO_4 + y M NaH_2PO_4 to be adjusted to either pH 6 0 or 8 0, (ii) 0 05 M Na_2HPO_4 + 0 1 M NaOH at pH 11 5 Solutions were prepared from twice-distilled water and A R chemicals, and purged in the cell with purified Ar for 1 h prior to each run

Preceding each run the working electrode was firstly potential cycled at 0 01 V s^{-1} between the hydrogen evolution reaction potential range to the Cu passivation potential range to obtain a reproducible voltammogram Cyclic voltammograms were recorded at 0 01 V s^{-1} between preset cathodic ($E_{s,c}$) and anodic ($E_{s,a}$) switching potentials and plotted by taking j, the current density referred to A, the geometric working electrode area, *vs* E, the applied potential Anodic current transients were presented as j *vs* time (t) plots in the phosphate buffers at a constant potential E_s In these cases, the working electrode has been previously held at the potential E_c for 3 min ($E_c < E_s$), a potential which is close to the HER threshold potential

SEM observations and EDAX of the electrochemically treated and blank specimens were made by using a Cambridge Stereoscan 150

3. RESULTS

3 1 *Voltammetric data*

3 1 1 *Phosphate buffer, pH* 6 The stabilized voltammogram of Cu specimens in this buffer solution was recorded at 0 01 V s^{-1} between $E_{s,c} = -0\,65$ V and $E_{s,a} = 0\,10$ V (Fig 1a) The positive potential going scan shows an anodic current starting at *ca* −0 2 V which defines a broad anodic current peak (peak I_a) at −0 02 V The anodic charge density (q_a) involved in peak I_a is 3 9 mC cm^{-2} The returning scan exhibits a single sharp cathodic peak (peak I_c) at −0 13 V with a small hump at its descending branch The cathodic charge density (q_c) corresponding to peak I_c is 2 6 mC cm^{-2}

The cyclovoltammograms show that the peak potential difference of peaks I_a/I_c decreases as $E_{s,a}$ is stepwise changed from −0 45 to 0 10 V, and simultaneously the cathodic hump disappears The fact that in the present case $q_a > q_c$ suggests that the electroformation of the anodic layer is presumably accompanied by the formation of soluble Cu^{2+} species during the electrooxidation scan

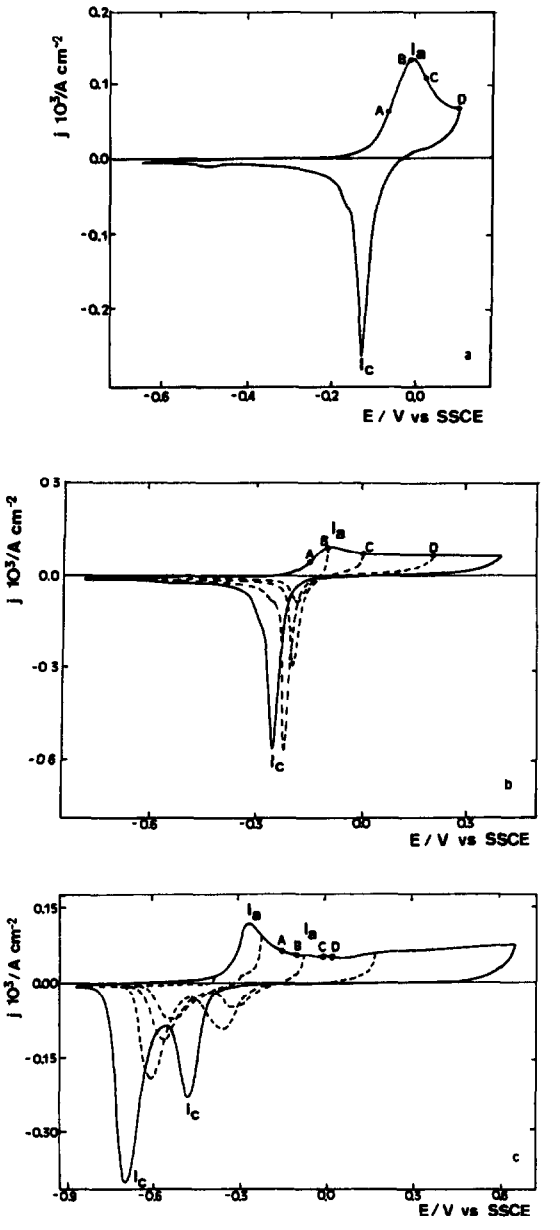

Fig 1 Voltammograms of annealed Cu electrodes in phosphate buffer solutions run at 0 01 V s^{-1}, (a) pH 6, (b) pH 8 and (c) pH 11 5 Points labelled A, B, C and D correspond to potential values at which the potentiostatic current transients were recorded

For peak I_a, the peak current, i_p, *vs* $v^{1/2}$ plot, approaches, in principle, two linear regions with a cross over at $v = 0\,02$ V s^{-1} (Fig 2) suggesting that there are two diffusion controlled processes operating on different time scales

Finally, the voltammogram also shows a very broad although small cathodic peak covering −0 45 to −0 50 V

3 1 2 *Phosphate buffer, pH* 8 The stabilized voltammogram of a Cu specimen in this solution run at 0 01 V s^{-1} between $E_{s,c} = -0\,80$ V and $E_{s,a} = 0\,40$ V is shown in Fig 1b The positive potential going scan presents peaks I_a and I_c at −0 10 and

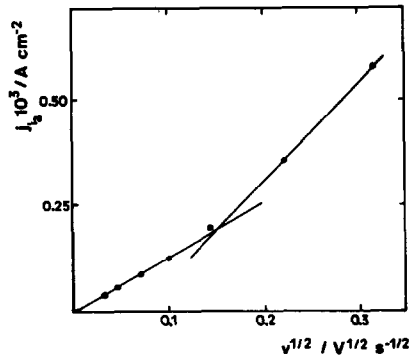

Fig 2 Current peak height j_{la} *vs* $v^{1/2}$ relationship in phosphate buffer at pH 6

$-0\,25$ V, respectively When $E_{s,a}$ is set in the $-0\,45$ to 0 40 V range, peak I_c looks very sharp. Likewise, an anodic current plateau extending from 0 05 V upwards can be observed In this case the anodic to cathodic charge density ratio approaches a value close to one ($q_a = 1\,18$ mC cm^{-2}, $q_c = 1\,17$ mC cm^{-2}) Nevertheless, the overall voltammetric charge decreases as the rotation speed (ω) of the working electrode is increased gradually from 0 to 3500 rpm, although one can note that the cathodic voltammetric charge decreases faster than the anodic one The latter is an indication that the entire electrochemical process involves a transport of soluble species related to the anodic reaction

The same minor contributions referred to in Section 3 1 1 are also seen in the voltammogram depicted in Fig 1b

3 1 3 *Phosphate buffer, pH* 11 5 The stabilized voltammogram of a Cu specimen in this buffer solution was run at 0 01 V s^{-1} between $E_{s,c} = -0\,86$ V and $E_{s,a} = 0\,65$ V (Fig 1c) The positive going scan exhibits a broad peak I'_a located at $-0\,28$ V, and at more positive potentials, a nearly constant anodic current Likewise, the negative potential going scan shows the cathodic current peaks I_c and I'_c at $-0\,49$ and $-0\,70$ V, respectively The voltammograms run between $E_{s,c} = -0\,86$ V and a value of $E_{s,a}$ progressively shifted in the positive direction reveal that the initial part of peak I'_a is related to peak I'_c, whereas the positive potential branch of the peak I'_a as well as the constant anodic current region appear to be related to both peaks I_c and I'_c These results are similar to those previously reported for Cu in alkaline solutions[22] From the latter it was concluded that a thin Cu(I) oxide was initially formed at lower potentials, and subsequently a hydrous Cu(II) oxide layer was produced at more positive potentials Thus, at pH 11 5 the initial part of peak I_a can be assigned to the electroformation of a Cu(I) oxide layer which can be electroreduced to Cu in the potential range of peak I'_c

On the other hand, the positive potential branch of peak I'_a as well as the constant anodic current region can be associated with the electroformation of a hydrous Cu(II) oxide layer which is electroreduced to Cu(I) oxide in the potential range of peak I_c. It can be noted that under comparable conditions with respect to pH 6 and 8, the following values result· $q_a = 1.1$ mC cm^{-2}, $q'_a = 1.5$ mC cm^{-2} and $q_c = 1\,0$ mC cm^{-2} and $q'_c = 1\,5$ mC cm^{-2}

3.2 *Anodic current transients in phosphate buffers at different pH*

In the phosphate buffer at pH 6 the anodic current transients at constant potential were run by stepping the potential to $E_c = -0\,35$ V for 3 min to attain the complete electroreduction of the Cu surface, and subsequently to E_s to record the corresponding current transient For values of E_s ranging between $-0\,07$ and 0 10 V the current transients exhibit only a monotonous decay to reach the corresponding stationary passivity current value without other particular features (Fig 3a) The i *vs* $t^{-1/2}$ plots at low E_s values give straight lines for $t > 0\,5$ s with a slope dependent on E_s (Fig 4)

Similar anodic current transients resulted at pH 8 and 11 5 (Fig 3b and c) In these cases the values of

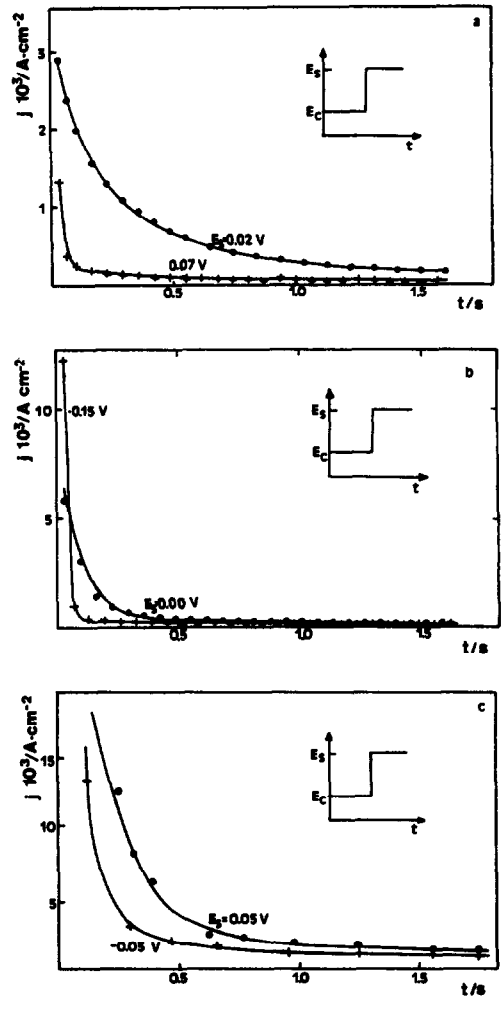

Fig. 3 Potentiostatic current transients for Cu electrodes in phosphate buffer, (a) pH 6, (b) pH 8 and (c) pH 11 5 The values of E_s are indicated in the figures The full trace corresponds to the theoretical function calculated from equations (12) and (13)

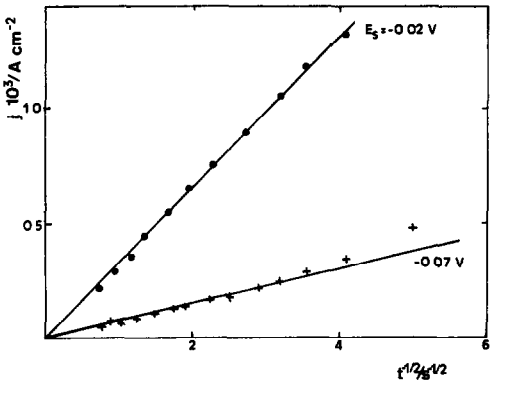

Fig 4 Transient current density j *vs* $t^{-1/2}$ plots at pH 6

E_c and E_s were conveniently adjusted, as shown in the corresponding figures

3 3 *SEM micrographs and EDAX data*

SEM micrographs were obtained at 400, 40 and 2 μm unit scale, for blank and electrochemically treated specimens The latter were held for 10 min at different potentials, namely, −0 80, −0 45 or −0 15 V in the solution at pH 11 5, −0 80, −0 20 or 0 15 V in the solution at pH 8, −0 75, −0 10 or 0 15 V in the solution at pH 6

The SEM micrographs of the blank exhibit at the 400 μm unit scale (Fig 5a) rounded grains which at a larger magnification (Fig 5b) present rounded micropits A detailed micrograph of one of these micropits (Fig 5c) which have been formed during Cu electropolishing, show a rounded morphology

The SEM micrographs of the Cu specimens anodized at −0 15 V and pH 11 5 (Fig 6) show a Cu surface similar to that seen for the blank (Fig 5)

The same results are found for Cu specimens treated at pH 6 and 8 and anodized to −0 80 and −0 20 V In contrast, for those specimens anodized at 0 15 V, the formation of a thin crystalline anodic layer can be seen at the highest magnification (Fig 7) This crystalline layer appears on the Cu specimens subjected to high positive anodization potentials at low pH

The EDAX covered different domains of the specimen surface including micropits For those electrodes anodized at potentials lower than the potential of peak I_a, the EDAX of the main surface domains indicates the major contribution of Cu, minor traces of Al and Si (Fig 8a) But for those specimens anodized at potentials more positive than the potential of peak I_a and low pH, the EDAX revealed the presence of P on the surface (Fig 8b)

On the other hand, the EDAX data inside the micropits reveals two interesting features Firstly, independently of the anodization conditions, all specimens show a relatively large concentration of Al and Si inside the pits Secondly, the EDAX data show no P signal inside the micropits, except for those specimens which were anodized at high positive potential and low pH, although in these cases, the amount of P was just within the limits of detection

4. DISCUSSION

4 1 *Preliminary considerations*

The electrochemical behaviour of polycrystalline Cu in aqueous solutions containing phosphate ions is rather complex as it involves at least two main processes, namely, the formation of soluble species and the onset of passivity caused by the growth of an anodic film both processes being pH dependent This conclusion is derived from the values of q_a and q_c, the voltammetric charges resulting from peaks I_a and I_c, respectively The value of q_a particularly under stirring, is greater than the value of q_c, the difference $\Delta q = q_a - q_c$ becomes smaller as the solution pH is shifted from 6 to 11 5 This result indicates that the formation of soluble species decreases considerably as the solution pH increases

For interpreting the experimental data it is convenient to consider the following equilibria under standard conditions[23, 24]

$$Cu^+ + e^- = Cu, \quad E^\circ = 0\,52\,V \ (nhe) \quad (1)$$

$$Cu^{2+} + e^- = Cu^+, \quad E^\circ = 0\,16\,V \quad (2)$$

$$Cu^{2+} + 2e^- = Cu, \quad E^\circ = 0\,34\,V \quad (3)$$

$$Cu^{2+} + H_2O = CuOH^+ + H^+, \quad pK_a = 7\,3 \quad (4)$$

$$2Cu^{2+} + H_2O = Cu_2O^{2-} + 2H^+, \quad pK_a = 10\,5 \quad (5)$$

$$Cu^+ + OH^- = CuOH, \quad pK_s = 14\,7 \quad (6)$$

$$Cu^{2+} + 2OH^- = Cu(OH)_2, \quad pK_s = 19\,9 \quad (7)$$

$$2PO_4^{3-} + 3Cu^{2+} = Cu_3(PO_4)_2, \quad pK_s = 36\,9 \quad (8)$$

$$H_3PO_4 = H^+ + H_2PO_4^-, \quad pK_{1a} = 2\,1 \quad (9a)$$

$$H_2PO_4^- = H^+ + HPO_4^{2-}, \quad pK_{2a} = 7\,2 \quad (9b)$$

$$HPO_4^{2-} = H^+ + PO_4^{3-}, \quad pK_{3a} = 12\,7 \quad (9c)$$

According to the potential and pK values of these reactions the composition of the anodic layer should depend on the phosphate concentration and solution pH Thus, at pH 6–8 basic Cu phosphates should be the main component of the passive layer These type of compounds are well known, covering a wide range of phosphate/hydroxide stoichiometries[24] This conclusion is consistent with EDAX data showing the presence of P on the surface of Cu specimens anodized at those pH (Fig 8b) The formation of this type of layers explains the single voltammetric electroreduction peak observed for Cu in phosphate buffer at pH 6–8

On the other hand, at pH 11 5, the characteristics of reactions (1)–(9) also indicate that the composition of the passive layer should change in the direction of increasing the contribution of Cu oxide and hydroxide species despite the fact that the phosphate ions are present in the solution Accordingly, the voltammetric behaviour of Cu actually reproduces that already described for Cu in plain alkaline solution[25], *te* the composition of the passive layer can be described as a Cu(I) oxide/hydrous Cu(II) oxide duplex layer structure

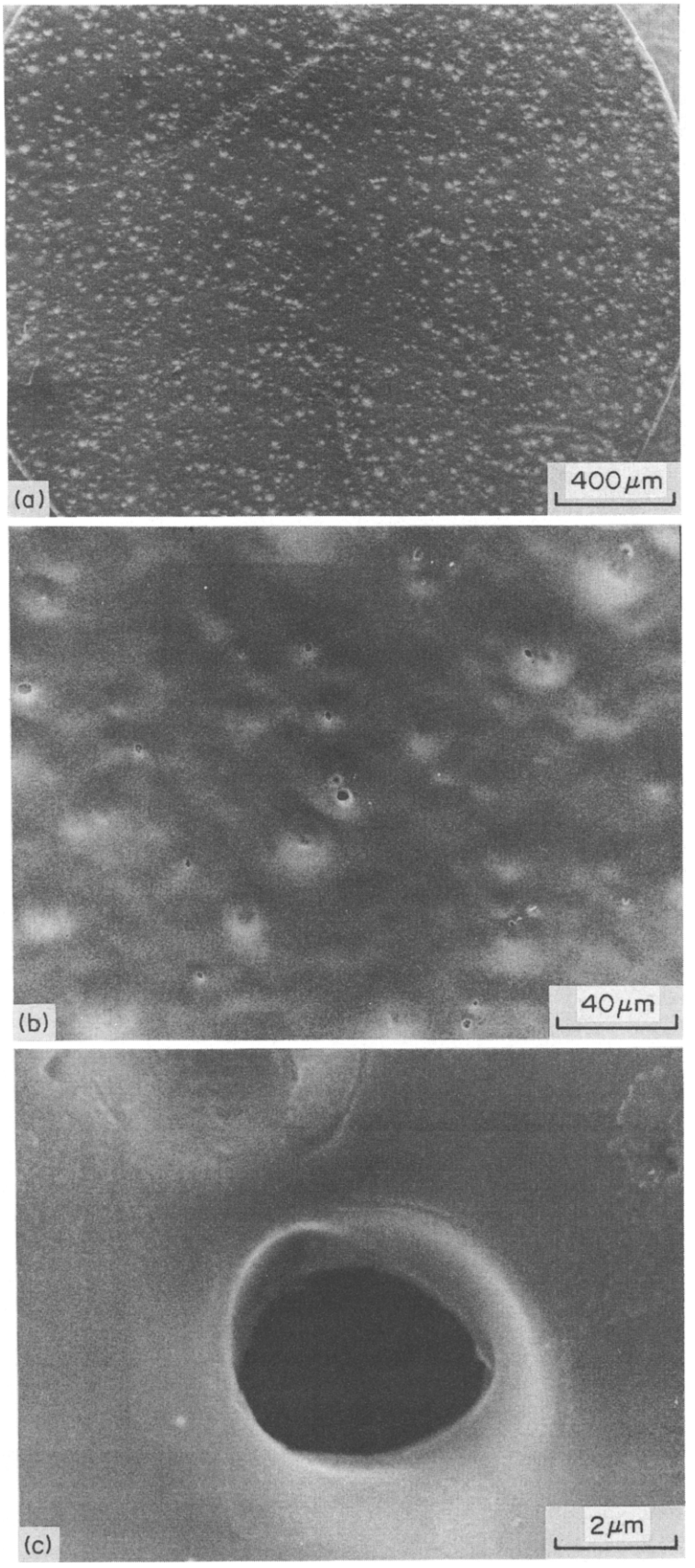

Fig 5 SEM micrographs of the Cu blank specimens obtained at different magnifications Bars correspond to 400 μm (a), 40 μm (b), and 2 μm (c)

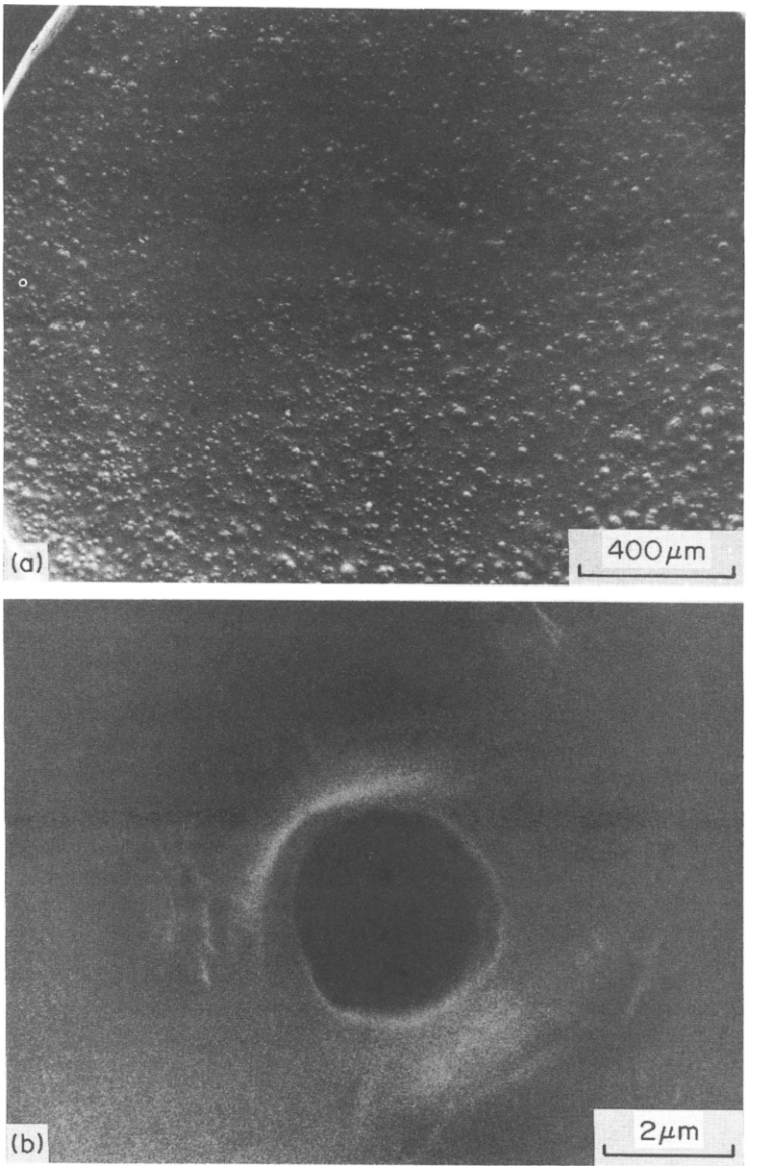

Fig 6 SEM micrographs at different magnifications of a Cu specimen anodized in the phosphate buffer, pH 11 5, $E_s = -0$ 15 V Bars correspond to (a) 400 μm and (b) 2 μm,

4 2 *Analysis of the anodic current transients*

The analysis of the anodic current transients obtained at constant potential offers the possibility of modelling the entire electrodissolution and passivation of Cu in the different phosphate containing solutions For this purpose, the model previously described for the passivity of Cu and other metals in alkaline solutions[26–28] can be used, due to the fact that the behaviour of the system at the highest pH resembles that already described for Cu in alkaline solutions Thus, the overall anodic current density, j_t, was expressed as the sum of three main contributions, namely, j_{dl}, the current density associated with the double layer charging, j_a, the current density related to Cu electrodissolution, and j_p, the current density related to the passive layer formation Thus

$$j_t = j_{dl} + j_a + j_p \tag{10}$$

Under the present conditions, the contribution of j_{dl} can be neglected because it disappears in a time range much shorter than that of other transient processes Accordingly, equation (10) can be written as

$$j_t = j_a + j_p \tag{11}$$

Hence, as a first approach one can describe the growth of the anodic layer as an instantaneous nucleation and 2D growth under diffusion control The corresponding rate equation is[29]

$$j_p = P_1 \exp(-P_2 t), \tag{12}$$

where

$$P_1 = q\pi KDN_0 \tag{12a}$$

$$P_2 = \pi KDN_0 \tag{12b}$$

$$P_1/P_2 = q \tag{12c}$$

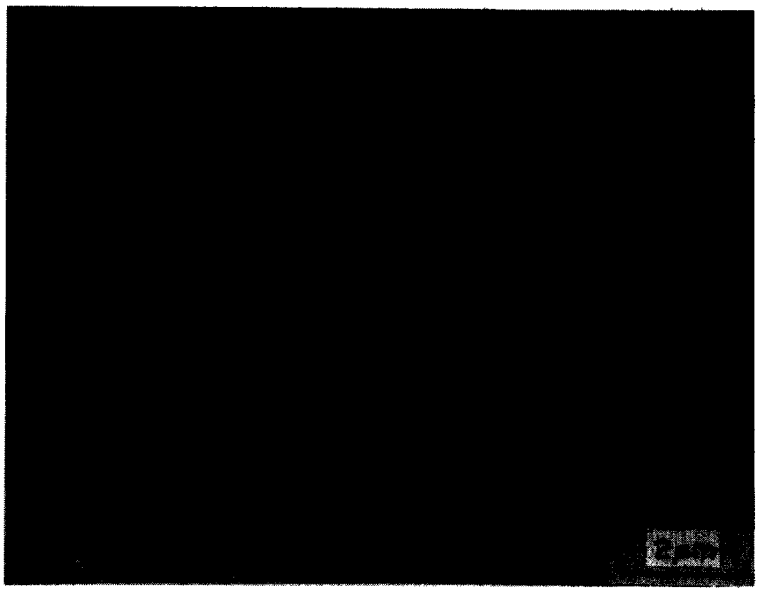

Fig 7 SEM micrograph of a Cu specimen anodized a pH 6 and $E_s = 0.15$ V Bar corresponds to 2 μm

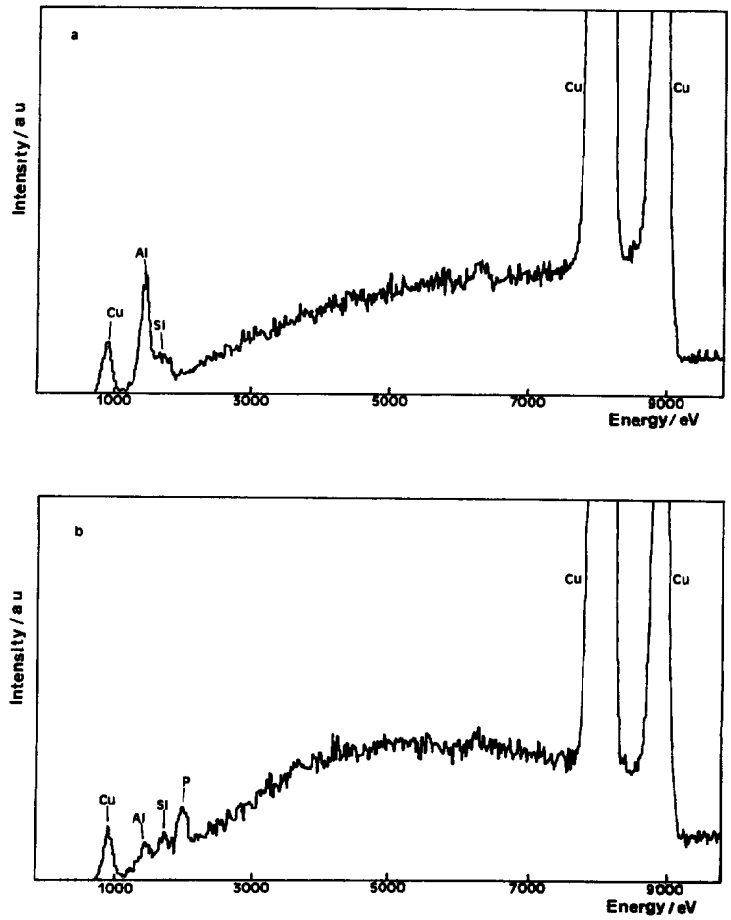

Fig 8 EDAX of Cu specimens anodized at different potentials (a) E_s more negative than the threshold potential of peak I_a, (b) E_s more positive than the threshold potential of peak I_a

Table 1 Parameters used in simulation of potentiostatic current transients with equations (12) and (13)

E_s/V	$P_1/P_2/10^6$ C cm^{-2}	$P_3/10^4$ A s$^{1/2}$ cm^{-2}	P_4/s^{-1}
	pH 6		
−0 07	9 41	0 38	0 132
−0 02	48	1 71	0 02
1 10	110	3 29	0 014
0 10	599	3 19	0 003
	pH 8		
−0 15	12 1	0 096	0 199
−0 10	71 5	0 831	0 078
0 00	267	2 48	0 053
0 20	419	1 42	0 040
	pH 11 5		
−0 15	163	0 62	1 55
−0 10	284	1 30	12 25
0 00	451	1 38	6 56
0 20	614	1 81	5 66

q is the charge density involved in the passive layer formation, K is a proportionality constant, D is the diffusion coefficient of the species involved in the passive layer growth, and N_0 is the number of sites available for nucleation

On the other hand, one can attempt to model the proper Cu electrodissolution as a nucleation and growth of 3D voids at certain sites of the metal surface under diffusion control For an instantaneous nucleation[30], the corresponding rate equation is

$$j_a = (P_3/t^{1/2})[1 - \exp(-P_4 t)], \quad (13)$$

where

$$P_3 = zFD'^{1/2}\Delta c'\pi^{-1/2} \quad (13a)$$

$$P_4 = \pi K' D' N_0', \quad (13b)$$

and the dashed symbols have the same meaning as before, except that now they refer to the conditions of the new model, and $\Delta c'$ is the concentration gradient created by the actual Cu electrodissolution process The presence of two different diffusional processes, in the short time range and in the long time range, respectively, is supported by the two linear portions shown in the i_p *vs* $v^{1/2}$ relationship (Fig 2)

By using equations (11)–(13) the current transients recorded at different stages of Cu electrodissolution and passivation at pH 6–11 5 (Fig 3a–c) can be reproduced with the set of parameters assembled in Table 1 These parameters contain valuable information on the processes under investigation The values of q, P_3 and P_4 corresponding to the potential values indicated by points A, B, C and D in the voltammograms shown in Fig 1 are shown in Table 1 At pH 6–8 the value of q becomes smaller than the single monolayer charge density value for points A, B, and C of the current peak I_a (Fig 9) However, q reaches the monolayer charge density value at point D, which rests in the net passive region On the other hand, at pH 11 5 the value of q reaches the monolayer charge density value already at point C in the voltammogram (Fig 1c)

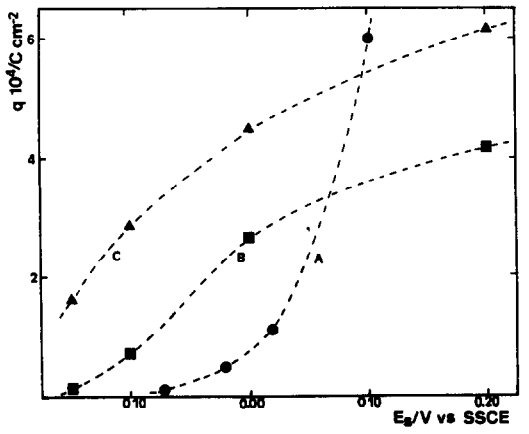

Fig 9 Dependence of q on E_s (A) pH 6, (B) pH 8, (C) pH 11 5

At a constant pH the decrease of P_4 reflects the change of N_0' with q according to the coverage and thickness of the passive layer Moreover, the fact that the micropit size does not change during the anodization allows us to discard the possibility that the sites for Cu electrodissolution could be identified with the micropits formed during the Cu electropolishing This conclusion emerges from the analysis of the SEM data

On the other hand, the potential dependence of P_3 reflects the influence of the potential on $\Delta c'$ and D' At potentials where the passivating layer is still incomplete, the value of $\Delta c'$ increase with the potential and the diffusion coefficient of Cu^{2+} ion in aqueous solutions should be considered Consequently, under these conditions the value of P_3 should increase the applied potential Conversely, at potentials where the passivating layer approaches completeness the main influence on P_3 comes out from the diffusion coefficient of Cu^{2+} ions through the passivating layer which should be smaller than the former one This implies that P_3 firstly increases rather sharply and later slightly decreases or remains nearly constant with the applied potential

At a constant potential the change of pH from 6 to 11 5 results in an increase of q as it should correspond for a gradual thickening of the inner passive layer Accordingly, at high positive potentials a decrease of P_3 is observed This fact agrees with the decrease observed in both q_a and q_c as the pH increases The high values of P_3 obtained at pH 11 5 can be associated with an increase of the N_0' value, probably due to the change in the chemical

composition of the inner passive layer from Cu(II) phosphate (pH 6–8) to a complex Cu(I)–Cu(II)–oxide–phosphate layer (pH 11 5)

From the physical picture of the proposed model, one should expect that at the beginning of Cu passivation the electrodissolution of the metal takes place mostly at the predominant passive layer-free areas. In this case, the passivating layer can be described as a number of thin islands covering only a small fraction of the total metal surface, the formation of these areas being initially relatively faster than the reaction producing soluble Cu species The formation of island-type structures has been recently demonstrated by *in situ* scanning tunneling microscopy for the electrochemical growth of the Au oxide layer on Au[31]

Otherwise, at the peak potential one should expect that about one half of the surface becomes already covered by islands of passivating species Then, the electrodissolution of Cu can occur either via the free metal surface or via the passivating layer covered area, although in this case the latter contribution may be considerably smaller than the first one

Finally, when the formation of the passive layer is complete, the electrodissolution of Cu should proceed only through the passivating layer and the electroformed Cu^{2+} soluble species can precipitate at the outer region of the passivating layer (layer thickening) This explanation is consistent with the relatively large values of q_c as compared to the value of q derived from the current transients because the former one involves the electroreduction of both the inner and the outer parts of the passivating layer

Hence, the precedent mechanistic model describes satisfactorily the kinetics of the complex processes related to the electrodissolution and passivation of Cu in phosphate containing solutions at pH 6 0–11 5 for different stages of Cu passivation

Acknowledgements—Financial support for this work by the Gobierno de Canarias (Dirección General de Universidades e Investigación) under contract No 46/01 06 88, is gratefully acknowledged Authors thank Prof S Trasatti and Mr G Terzaghi, Centro de Microscopia Elettronica del Dipartamento de Chimica Fisica ed Elettrochimica dell'Universita di Milano for making available SEM and EDAX facilities

REFERENCES

1 T P Hoar and G P Rothwell, *Electrochim Acta* **9**, 135 (1964)
2 T P Hoar and T W Farthing, *Nature* **169**, 324 (1952)
3 M C Petit, *Electrochim Acta* **8**, 217 (1963)
4 B Pointu, *Electrochim Acta* **14**, 1207 (1969)
5 B Pointu, *Electrochim Acta* **14**, 1213 (1969).
6 P Poncet, M Braizaz, B Pointu and J Rousseau, *J Chim Phys* **75**, 287 (1978)
7 G H Sedahmed, M Z El-Abd, I A S Mansour, A M Ahmed and A A Wragg, *J appl Electrochem* **9**, 1 (1979)
8 K Kojima and C W Tobias, *J electrochem Soc* **120**, 1026 (1973)
9 J A Allen, *Trans Faraday Soc* **48**, 273 (1952)
10 E C Williams and M A Barrett, *J electrochem Soc* **103**, 363 (1956)
11 M Novak and A Szucs, *J electroanal Chem* **210**, 237 (1986)
12 M Novak, A K Reddy and H Wroblowa, *J electrochem Soc* **117**, 733 (1970)
13 K Ohashi, T, Murakawa and S Nagaura, *J electrochem Soc Jpn* **30**, 165 (1962)
14 K Kojima and C W Tobias, *J electrochem Soc* **120**, 1202 (1973)
15 M Novak and A Szucs, *J electroanal Chem* **210**, 229 (1986)
16 B Pointu, M Braizaz, P Poncet, J Rousseau and N Muhlstein, *J electroanal Chem* **122**, 111 (1981)
17 B Pointu, M Braizaz, P Poncet and J Rousseau, *J electroanal Chem* **151**, 65 (1983)
18 B Pointu, M Braizaz, P Poncet and J Rousseau, *J electroanal Chem* **151**, 79 (1983)
19 A Szucs and M Novak, *J electroanal Chem* **210**, 247 (1986)
20 D Dickertmann, F D Koppitz and J W Schultze, *Electrochim Acta* **21**, 967 (1976)
21 J M Sánchez-Marín and J M Las Heras, *Conocimiento de Materiales* (in Spanish), Ch 44 Editorial Donostiarra, San Sebastián, Spain (1982)
22 H D Speckmann, M M Lohrengel, J W Schultze and H H Strehblow, *Ber Bunsenges Phys Chem* **89**, 392 (1985)
23 *Encyclopedia of Electrochemistry of the Elements*, Vol II (Edited by A J Bard) Marcel Dekker, New York (1976)
24 P Pascal, *Noveau Traité de Chimie Minérale*, Vol III, p 344 Masson et Cie, Paris (1957)
25 D V Vásquez Moll, M. R G de Chialvo, R C Salverezza and A J Arvia, *Electrochim Acta* **30**, 1011 (1985)
26 M R G de Chialvo, D V Vásquez Moll, R C. Salverezza and A J Arvia, *Electrochim Acta* **30**, 1501 (1985)
27 R C Salvarezza, D V Vásquez Moll and A J Arvia, *Electrochim Acta* **32**, 1421 (1987)
28 D V Vásquez Moll, R. C Salvarezza, H Videla and A J Arvia, *J electrochem Soc* **132**, 754 (1985)
29 W Davison and J A Harrison, *J electroanal Chem* **44**, 213 (1973)
30 B Scharifker and G Hills, *Electrochim Acta* **28**, 879 (1983)
31 R J Nichols, O M Magnussen, J Hotlos, T Twomey, R J Behm and D M Kolb, *J electroanal Chem* **290**, 21 (1990)